



Analysis of the response of the Epitácio Pessoa reservoir (Brazilian semiarid region) to potential future drought, water transfer and LULC scenarios

Jorge Flávio Casé Braga da Costa Silva¹ · Richarde Marques da Silva² · Celso Augusto Guimarães Santos³ · Alexandro Medeiros Silva¹ · Pedro Costa Guedes Vianna²

Received: 15 November 2020 / Accepted: 3 April 2021 / Published online: 17 April 2021
© The Author(s), under exclusive licence to Springer Nature B.V. 2021

Abstract

The Brazilian semiarid region (BSAR) is affected by the high precipitation variability and severe drought events over time, promoting recurrent water scarcity. The water supply in the BSAR has suffered since 2012 from severe incidents of rainfall reduction, creating a complex scenario of water scarcity, for instance, in Campina Grande city, which is supplied by the Epitácio Pessoa reservoir (EPR). This study analyzed the future impacts on the volume of the EPR based on potential future droughts, water transfer from the São Francisco River, population growth and recent changes in land use and land cover (LULC). Several procedures were performed, including (a) simulation of LULC scenarios with the LCM algorithm, (b) simulation of future rainfall scenarios for the period from 2020 to 2030, (c) streamflow simulation using the Soil Water and Assessment Tool (SWAT) model and (d) prediction of water storage in the EPR for the period from 2020 to 2030 using three rainfall scenarios (– 40%, – 45% and – 50%). The results indicated that the SWAT calibration and validation results were considered satisfactory based on the R^2 , Nash, and PBIAS values. The results were assumed from the rainfall scenarios for the period from 2020 to 2030 together with the LULC scenario for 2030, including the estimated outflow of water transfer from the São Francisco River. The results showed, based on the three adopted rainfall scenarios, that the reservoir would reach its critical volume in the first two years of the analyzed period, and the reservoir volume would then increase until 2024 and subsequently return to decrease, reaching the critical volume in 2030.

✉ Celso Augusto Guimarães Santos
celso@ct.ufpb.br

¹ Postgraduate Programme in Geography (CCEN), Federal University of Paraíba, João Pessoa, PB 58051-900, Brazil

² Department of Geosciences, Federal University of Paraíba, João Pessoa, PB 58051-900, Brazil

³ Department of Civil and Environmental Engineering, Federal University of Paraíba, PB, João Pessoa 58051-900, Brazil

Graphical Abstract



Keywords Modeling · GIS · Remote sensing · Drought · Future scenarios · Water scarcity

1 Introduction

In Brazil, drought is one of the most serious natural disasters, reaching millions of people in the Brazilian semiarid region (BSAR). In addition, this phenomenon is complex, important and extremely recurrent in the region (Dos Santos et al. 2020). The BSAR is one of the most populous semiarid areas in the world, where water supply has become a major problem (Santos et al. 2019a). BSAR has always faced periods of drought in recent centuries due to the irregular spatial distribution of precipitation, geology and soil types in the region (Marçal et al. 2019). Droughts cause many problems in the daily lives of the population of this region, as they affect the entire society, harming economic and social development (Tomasella et al. 2018). Considering drought as a recurring natural disaster in the BSAR, its occurrence compromises the water security of agriculture and the supply of urban areas, increasing population poverty and economic crisis (Cunha et al. 2018). Droughts associated with other processes, such as intensive land use and poor natural resource management policies, cause socioenvironmental impacts of varying magnitudes, such as desertification, soil aridity and reduced agricultural potential (Silva et al. 2018a). The BSAR is considered the most vulnerable area to drought in Brazil. Among the main variables that contribute to this water scarcity scenario are climatic variability, high evapotranspiration, increased demand per capita for water, changes in land use and land cover (LULC) and problems with water management. This combination of factors makes the BSAR one of the most vulnerable regions in the world to precipitation variability (Coelho et al. 2018).

Regarding the influence of climatic variation in semiarid regions, studies by Bacalhau et al. (2016), Pereira et al. (2018) and Marengo et al. (2018) have highlighted that over the long term, the projected rainfall deficits in BSAR together with the increased temperatures and more recurrent droughts and dry spells can aggravate environmental degradation. In this sense, the future impacts of climate change on semiarid regions can intensify and prolong droughts in addition to causing serious problems, such as water scarcity and collapse of the water supply (Pes et al. 2017). In this sense, it is increasingly necessary to carry out hydrological forecasting studies in conjunction with public planning policies to face the

problems arising from extreme weather events (Braga et al. 2015). However, it is necessary to understand the uncertainties within these processes.

Studies on the performance sensitivity and estimation of the volume of reservoirs with various forecast management schemes for historical and future climatic scenarios using hydrological modeling, such as those performed by Yao and Georgakakos (2001), Celeste and Billib (2009), Tian et al. (2021), Umar et al. (2021), and Wu et al. (2021), are important for the management of water resources. These studies are even more important for reservoirs located in semiarid regions that are more susceptible to climatic variability (Martins et al. 2019), as is the case of the Epitácio Pessoa reservoir (EPR), which is located in BSAR, more precisely in Paraíba State, one of the poorest states in Brazil. This reservoir is the unique water source for a population of more than 500.00 inhabitants, and mainly for Campina Grande city, one of the largest cities in the BSAR. During 2012–2017, an extreme drought fell upon the EPR basin, causing the critical water storage condition of this reservoir that supplies Campina Grande (Brito et al. 2021; Silva et al. 2020b; Brasil Neto et al. 2021), the second largest city in Paraíba State with more than 411,000 inhabitants in 2020. This caused the reservoir to reach only 3.6% of its capacity in March 2017, resulting in the biggest crisis in the water supply of the last decades. Among the factors that contributed to this crisis can be highlighted the lack of an adequate management of water resources, the adoption of rationing policies only in moments of crisis containment and the decrease in the precipitated volume in that period. This emphasizes the need for effective management of this reservoir based on prediction of future drought scenarios. Thus, decision makers based on such predictions will be able to assess the potential impacts of different drought scenarios on the streamflow and water storage in the EPR.

Since May 2017, Campina Grande city and the EPR basin have been supplied with the water transfer from the São Francisco River Integration Project—PISF (Dantas et al. 2020). This project is intended to transfer water from the São Francisco River basin to small basins in northeastern Brazil. Concerns and benefits over the economic and social impacts of these water transfers exist at a regional scale, and therefore, should be studied from a holistic perspective involving hydrological modeling, LULC prediction, reservoir operation and drought scenarios. Thus, this study analyzed the future impacts on the

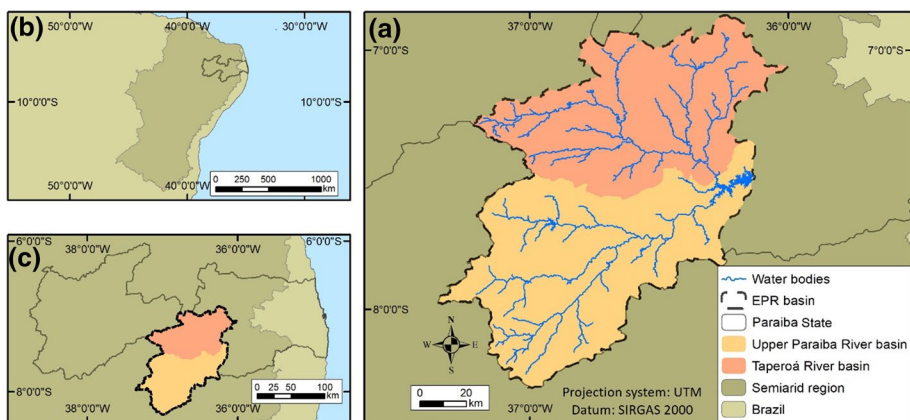


Fig. 1 Geographic location of the **a** Epitácio Pessoa reservoir basin, **b** Brazilian semiarid region and **c** Paraíba State

volume of the EPR based on potential future droughts, water transfer, population growth and recent changes in LULC in a semiarid region of Brazil.

2 Materials and methods

2.1 Research area and conceptualizing the study

This study was developed in the EPR basin. This basin has a total area of approximately 13,828 km² and is formed by the Upper Paraíba River basin and Taperoá River basin (Fig. 1). The EPR basin is located in the BSAR within Paraíba State, more precisely between the coordinates 36°00' and 37°30' W and 6°30' and 8°30' S (Fig. 1).

The average annual rainfall in the basin is approximately 600 mm, and the rainfall is irregularly distributed over time (Silva et al. 2020b). The Köppen climate classification is the Bsh type—low latitude and altitude (Alvares et al. 2013). The average monthly temperature is approximately 26 °C, with 2800 annual sunshine hours on average and a potential annual evapotranspiration of approximately 1100 mm (De Medeiros et al. 2019). The basin's geology is mainly composed of crystalline rocky substrate from the Precambrian period and intermittent and ephemeral rivers. The hydrography of the basin is considered poor in several aspects, with insufficient water conditions to supply the streamflow of rivers during long periods without precipitation. The region's rivers and reservoirs are irregular, with intermittent characteristics; the surface water disappears during the dry season, which has periods of well-defined seasonal drought (Souza et al. 2009). Regarding vegetation, the study area is located entirely in the Caatinga biome, which is characterized by deciduous species and spiny plants that are well adapted to the climatic conditions (Beuchle et al. 2015).

The EPR, which is located in this region and is popularly known as “Boqueirão,” is the second largest reservoir in terms of water storage capacity in Paraíba State. This reservoir was built between 1951 and 1956 by the National Department of Works Against

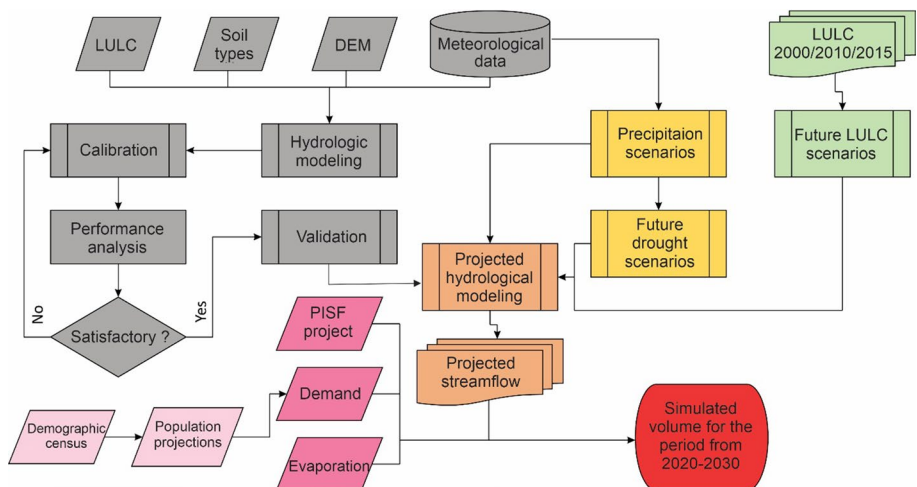


Fig. 2 Flowchart of the procedures performed in this study

Drought (DNOCS) with the initial objective of generating electricity and providing water for agricultural irrigation (SEMARH 2004). After its inauguration, several uses were integrated into the reservoir, such as supplying water to the municipality of Campina Grande and regularizing the Paraíba River as well as providing water for fishing activities, animal drinking, and sports and leisure practices (Brito 2013). To analyze the impacts of climatic, population and environmental variability on water availability between 2020 and 2030 in the EPR basin, a set of techniques, products and analyses were applied in this study, as shown in Fig. 2.

2.2 Population projections between 2020 and 2030

Population growth is a complex process of change that transforms nonurban areas into urban areas and influences economic and environmental issues. To analyze population projections from 2020 to 2030, historical population data from the municipalities that are supplied by the EPR were used. In this study, the IBGE demographic census surveyed in 1970, 1980, 1991, 2000 and 2010 (Silva 2019) provided the population-derived data aggregated by census boroughs for all basin, as proposed by de Espindola et al. (2017). The census borough is an administrative boundary defined by IBGE as the smallest territorial unit formed by a continuous area, fully contained in an urban or rural region, with a size suitable for the surveying interviews in each period (IBGE 2021). Population analysis was based using IBGE demographic census data, more precisely the total resident population in the households located in urban area in each census borough grouped for municipality, as the rural population is not served by the EPR. The urban population estimate of all municipalities within the basin was performed based on linear regression for the period from 2020 to 2030. This method admits that the population varies linearly with time and is used for short periods between 5 and 10 years, as proposed by Xie et al. (2018).

2.3 LULC mapping

In this study, LULC maps from 2000, 2010 and 2015 were used. These data were obtained from MapBiomias Project (MapBiomias 2019a, b) and are available at <http://mapbiomas.org>. The maps were produced from the classification pixel to pixel of images from Landsat satellites (30 m spatial resolution) using machine learning algorithms on the Google Earth Engine platform. Recently, MapBiomias Project has proposed to carry out the annual fully automatic mapping of all Brazilian biomes using Landsat images, obtaining good results (Parente et al. 2017; Bendini et al. 2019; Wang et al. 2019).

The Caatinga biome mapping was redefined to minimize the confusion between different natural vegetation and some LULC due to the difficult to classify vegetations with typical phenological behavior. In this study, some changes were made in the classified images acquired from MapBiomias to group some LULC classes. Due to the uncertainties and criteria of MapBiomias to classify the LULC in the Caatinga biome, a re-classification was performed based on Millington et al. (2021). Thus, the LULC classes of the original maps were simplified into five LULC classes, namely Caatinga vegetation, agriculture/pasture, built-up area, barren soil and water. To validate the classification, a set of points were collected through visual interpretation and checked with field trips.

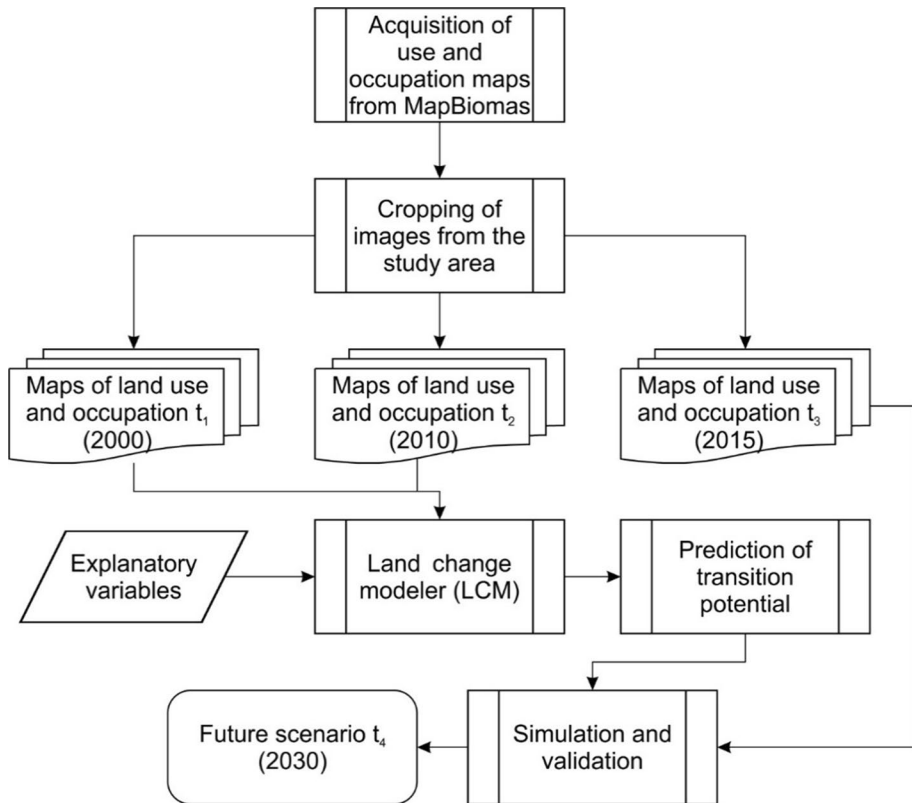


Fig. 3 Procedures used in mapping and predicting LULC scenarios

2.4 Simulation of LULC scenarios

The land change modeler (LCM) (Eastman 2016) was used to model the future LULC scenario for the EPR basin. The LCM provides a good understanding of the functions that describe changes in LULC (Silva et al. 2020a). The LCM model uses neural networks and Markov chains to analyze transition patterns through the provided maps and explanatory variables (Calijuri et al. 2015). This model has been used in several studies, such as Khawaldah (2016), Anand et al. (2018), Mas et al. (2014), and Olmedo et al. (2015). More details on the methodological procedures for LCM can be seen in Silva et al. (2020a). In this study, the LULC maps from 2000 (t_1), 2010 (t_2) and 2015 (t_3) were used to estimate the LULC in 2030 (t_4).

Figure 3 presents the flowchart used in the prediction of LULC for t_4 (2030) for the EPR basin using the LCM; the method basically consisted of the transition between potential forecasting steps, explanatory variables and simulation and validation of the LULC. The explanatory variables correspond to the factors that can influence LULC changes in the basin. In this study, the main explanatory variables that influence the trend of changes were (a) distance from highways, (c) distance from rivers and reservoirs, (c) urban areas, (d)

slope and (e) elevation. To assess the variables that most influence the process of LULC changes, the LCM model uses the Cramer test to elect and select the explanatory variables. This test is based on a nonparametric statistical analysis used to measure the strength of the association between variables that influence LULC changes (Silva et al. 2020a), and the explanatory variables can be associated with the defined transitions. Cramer test is obtained by Eq. 1 (Liebertrau 1983):

$$V = \sqrt{\frac{\chi^2}{n(q - 1)}} \tag{1}$$

$$\chi^2 = \frac{(O - E)^2}{2} \tag{2}$$

where V is the Cramer’s index, X^2 is the Chi-square coefficient, n is the sample size, q is the smallest value in the rows and columns of the image of the land cover, O is the observed frequency for a category, and E is the expected frequency in the corresponding category. V varies between 0 and 1, and the closer V is to 1, the larger is the association between the explanatory variable and the defined transition classes. If the V value is greater than 0.15, it demonstrates that the variable is significant for modeling and must be added in the transition potential forecast stage (Islam et al. 2018). Thus, only explanatory variables with V values greater than 0.15 were used to predict the LULC changes within the study area.

Table 1 Rainfall, streamflow and meteorological stations used in the study

Code	Name	Type	Longitude	Latitude	Altitude
736008	Soledade	Rainfall	– 36.37	– 7.07	560
736009	Serra Branca	Rainfall	– 36.67	– 7.48	450
736011	São José dos Cordeiros	Rainfall	– 36.82	– 7.38	610
736014	Pocinhos	Rainfall	– 36.07	– 7.07	624
736016	Gurjão	Rainfall	– 36.48	– 7.27	480
736017	Coxixola	Rainfall	– 36.62	– 7.62	465
736018	Congo	Rainfall	– 36.67	– 7.80	500
736020	Caraúbas	Rainfall	– 36.52	– 7.72	460
736021	Camalaú	Rainfall	– 36.87	– 7.92	565
736022	Cabaceiras	Rainfall	– 36.28	– 7.60	390
736025	Barra de São Miguel	Rainfall	– 36.33	– 7.75	520
737004	Prata	Rainfall	– 37.10	– 7.68	600
737018	Desterro	Rainfall	– 37.10	– 7.28	590
38830000	Caraúbas	Streamflow	– 36.50	– 7.72	493
38850000	Poço de Pedras	Streamflow	– 36.43	– 7.40	430
82890	Arcoverde	Meteorological	– 37.05	– 8.43	680
82792	Monteiro	Meteorological	– 37.06	– 7.88	603
82791	Patos	Meteorological	– 37.26	– 7.01	249
82795	Campina Grande	Meteorological	– 35.88	– 7.21	547

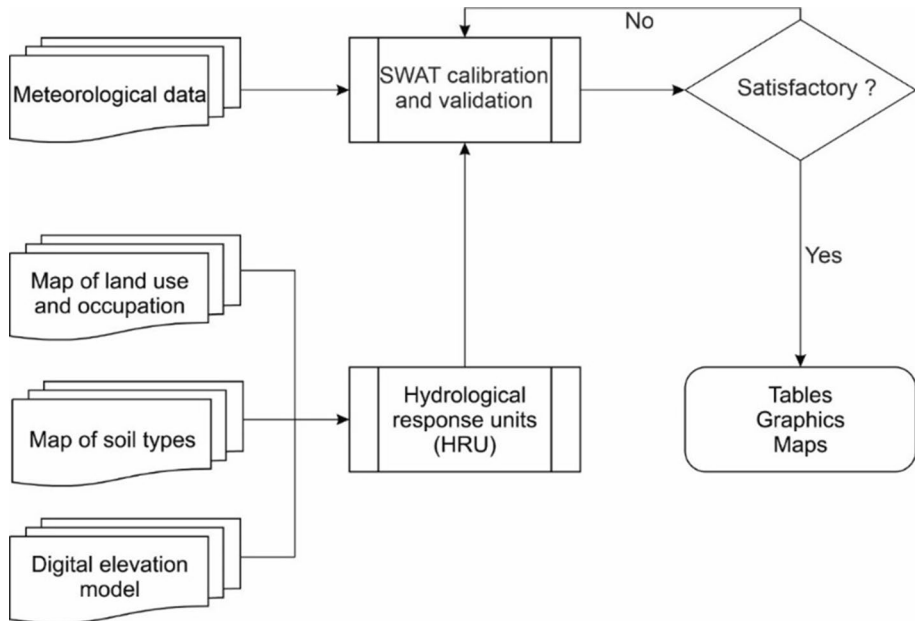


Fig. 4 Synthetic diagram of the steps that make up the SWAT model

2.5 Dataset and SWAT set up

To analyze precipitation and streamflow, data from January 1978 to December 1991 from 29 rain gauges and two streamflow gauges were used (ANA 2018). Meteorological data were acquired from the National Institute of Meteorology related to the period from 1978 to 1991 (INMET 2018) (Table 1). The streamflow time series of these stations were used in the calibration and validation processes of the Soil Water and Assessment Tool (SWAT) model (Arnold et al. 1998). The SWAT model is a comprehensive, semi-distributed multi-parameter hydrologic model and is one of the most used models for modeling runoff. This model divides the basin into subbasins based on relief, soil and LULC, and follows the procedures shown in Fig. 4.

To use the SWAT model, it is necessary to feed the database with geospatial information from the study area, such as the digital elevation model, soil type map and LULC map. Later, tabular data with the climatic conditions of the area are provided to the model. Figure 5a presents the description and spatial distribution of the rainfall gauges, streamflow stations and meteorological stations used in this study. For terrain modeling, imagery from the Advanced Spaceborne Thermal Emission and Reflection Radiometer—Global Digital Elevation Model (ASTER-GDEM) (Fig. 5b) with a resolution of 30 m was used, which is available at http://gdemdl.aster.jspacesystems.or.jp/index_en.html. The LULC information for the basin was obtained from the MapBiomas image from 2000 (Fig. 5c). Figure 5d shows the spatial distribution of soil types obtained from the Brazilian Soil Information System (EMBRAPA 2018), which provides a spatial database with information on Brazil's

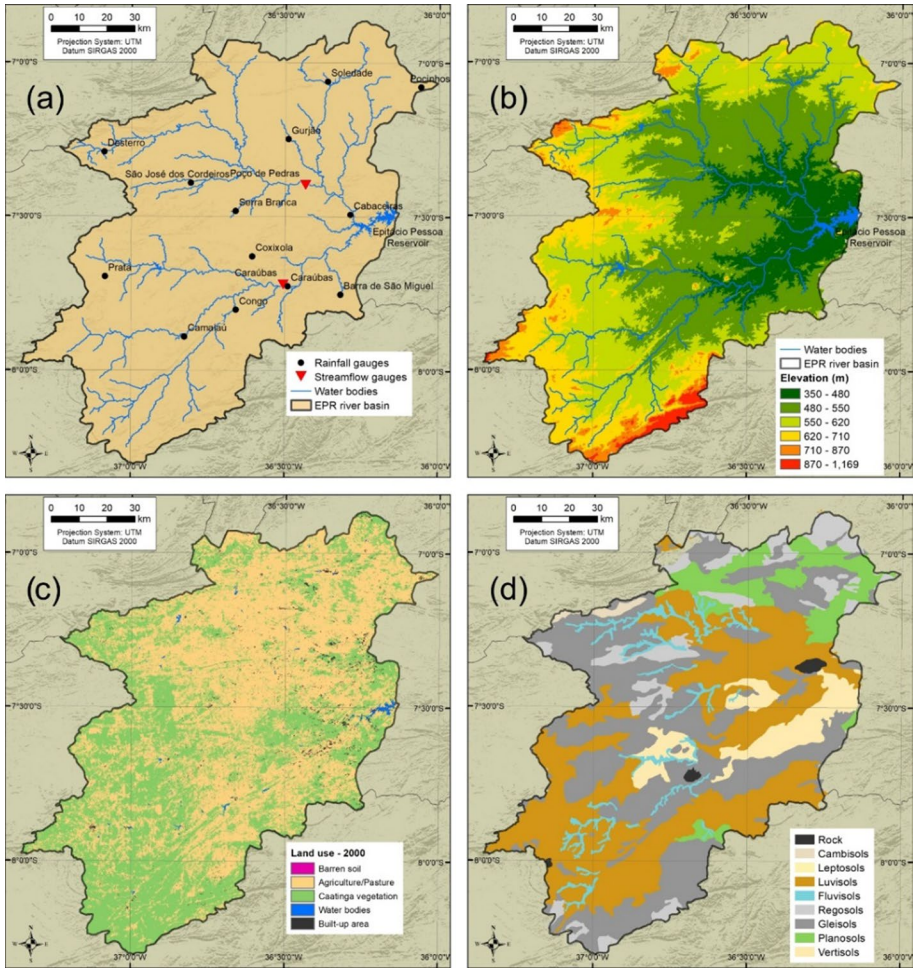


Fig. 5 a Precipitation and streamflow stations, b altimetry, c LULC and d types of soil existing in the EPR basin

soils. Subsequently, the climate information with a monthly scale was inserted into the SWAT.

2.6 Calibration, validation and performance evaluation of the SWAT model

The SWAT model was semiautomatically calibrated using the Sequential Uncertainty Fitting procedure, named SUFI-2 (Abbaspour et al. 2015), which is available in the SWAT Calibration Uncertainty Procedures (SWAT-CUP) software (Abbaspour et al. 2007). The model was calibrated for monthly streamflow based on data from two streamflow gauges, i.e., Caraúbas and Poço de Pedras, using a split sample test: three years for warm-up (1975–1977), the 1978–1988 period for calibration, and the 1992–1995 period for validation. In this study, 15 parameters (Table 2) were chosen

Table 2 Description of parameters automatically calibrated by SWAT-CUP

Parameter	Description	Initial value	Adjustment variation		Adjustment value ^c
			Method ^b	Minimum Maximum	
CN2 (dimensionless)	Curve number for normal antecedent moisture conditions	S ^a	%	± 20%	− 10.45%
Slsbbsn (m)	Average slope length	S	%	± 30%	+ 8.75%
Sol_AWC (mm/mm)	Soil available water capacity	S	%	± 30%	+ 15.89%
Sol_K (mm/h)	Saturated hydraulic conductivity	S	%	± 30%	− 28.47
Sol_Z (mm)	Depth from soil surface to bottom of layer	S	%	± 30%	+ 7.67%
Gwqmn (mm)	Threshold depth of water in the shallow aquifer required for return flow to occur	0	=	0	683.4
Canmx (mm)	Maximum canopy storage	0	=	0	7.652
Alpha_BF (days)	The baseflow recession constant	0.048	=	0	0.2817
Gw_Revap (dimensionless)	Groundwater “revap” coefficient	0.02	=	0.02	0.2651
Ch_N(2) (dimensionless)	Manning’s value for the main channel	S	=	0	9.47
Epc0 (dimensionless)	Plant uptake compensation factor	S	=	0.01	0.602
Esco (dimensionless)	Soil evaporation compensation coefficient	S	+	0.5	0.82
Revapmn (mm)	Threshold depth of water in the shallow aquifer or percolation to the deep aquifer to occur	S	+	− 1000	− 287
Ch_K(2) (mm/hr)	Effective hydraulic conductivity in main channel	0	+	− 0.01	0.045
Surlag (dimensionless)	Surface runoff lag coefficient	0	+	0.01	4.51

^aS varies spatially, because is related to each LULC and slope

^bThe methods used are (a) percentage method “%,” when the adjustment value varies in percentage in relation to the initial values of the parameters that varies spatially, (b) equality method “=,” when the initial value of the parameters are replaced by the adjustment value obtained after the calibration step, and (c) addition method “+,” when the value defined after the calibration step is added to the initial value of the parameter

^cThese are the variations obtained for each parameter after the calibration phase, which are applied to the initial values of each parameter

for optimization based on Silva et al. (2018b), Andrade et al. (2018), De Medeiros et al. (2019), and Santos et al. (2021). The results of the streamflow simulations were calibrated to maximize the R^2 , Nash–Sutcliffe efficiency (Nash) and percentage trend coefficient (PBIAS), based on Moriasi et al. (2007).

2.7 Statistical analysis of hydrological modeling performance

To compare the observed and simulated flows, three statistical methods were used: the Nash–Sutcliffe efficiency coefficient (Nash) (Nash and Sutcliffe 1970), the Pearson determination coefficient (R^2) and the percentage trend coefficient (PBIAS). These methods have already been used in several studies (Abbaspour et al. 2015; Golmohammadi et al. 2017; Moriasi et al. 2007; Pereira et al. 2016).

2.8 Water transfer from São Francisco River Integration Project (PISF)

PISF is a large water project in Brazil with 477 km in length, divided into two axes, the North and the East (Dantas et al. 2020). The objective of the PISF is to ensure the demand for water in areas of the BSAR that suffer most from irregular rainfall patterns and prolonged periods of drought (Brasil 2021). This project will benefit approximately 12 million people in 390 municipalities in the states of Pernambuco, Paraíba, Ceará and Rio Grande do Norte (Dantas et al. 2020). PISF is divided into those two major axes, which are composed by artificial canals, water pumping stations, reservoirs and hydroelectric plants for self-supply (Brasil 2004).

The axis of the PISF that supplies the EPR is the East axis. This stretch begins in the Itaparica reservoir, municipality of Floresta, in Pernambuco State. With a difference in level of 304 m along the stretch, the waters from the São Francisco River cover a total of 220 km. The East axis of the PISF has its entrance, in Paraíba State, in the Paraíba River basin, with the objective of this river perennation, to provide water security to the existing reservoirs along its course and to the EPR. With the arrival of the PISF waters, the reservoirs within this basin should have their levels stabilized, to guarantee the supply to the local population. The maximum flow is estimated at approximately 28 m³/s, with a minimum continuous flow around 10 m³/s. However, in practice, the flow that reaches the Paraíba River is approximately 3.60 m³/s (Dantas et al. 2020), and less than this value can reach the EPR due to water losses and upstream reservoirs along the main channel.

2.9 Simulation of future precipitation scenarios and EPR volume

To generate future rainfall projections for the period from 2020 to 2030, three daily rainfall of synthetic time series related to the 29 selected rain gauges were used. These three synthetic series were generated based on rainfall reductions from the period from 1978 to 1991, i.e., a decrease of 40%, 45% and 50% in relation to the average daily rainfall for each rain gauge used. Thus, three future rainfall scenarios in the basin were analyzed: (a) scenario 1: a 40% reduction in rainfall, (b) scenario 2: a 45% reduction in rainfall and (c) scenario 3: a 50% reduction in rainfall. This period and these pessimistic scenarios were chosen based on the results of the trend, slope and change-point detection tests presented

by Silva et al. (2020b), who identified the behavior of precipitation in the EPR basin and highlighted that this period has the greatest variability of rainfall. In addition, these climatic scenarios were chosen to analyze the behavior of the volume stored in the EPR during extreme future scenarios, as the drought that occurred from 2012 to 2017 in the region (Ferreira da Silva et al. 2020), which may affect water security in the region’s water supply, even with the arrival of water transfer from the São Francisco River. In this sense, a period that represented years with extreme rainfall and long periods of drought was chosen instead of data from climate projections generated by atmospheric circulation models.

After generating the rainfall scenarios, simulations were performed in the SWAT for each rainfall scenario, thus generating monthly flows for each of the three climatic scenarios. Subsequently, the results of the population projection for the 2020–2030 period were analyzed, which defined the demand for the human water supply by taking into account the per capita consumption values adopted by the Paraíba Water and Sewage Company (CAGEPA) (AESA 2018). Another factor used to simulate the future volume of the reservoir was the monthly evaporation data. In this study, the evaporation values were obtained from Oliveira et al. (2005), who analyzed the evaporation for the EPR.

The estimated volume in the reservoir for January 1, 2020, was 94,288,578.96 m³ (22.90% of the total storage capacity of the reservoir), according to AESA (2019). Subsequently, the mean streamflow of the Integration Project of the São Francisco River (PISF) was included and a constant value of 3.63 m³/s was assumed. After this stage, the streamflow estimated by the SWAT model was added, and the estimated volumes of the public supply and evaporation were removed each month, resulting in the volume stored in the reservoir. To perform the future simulation of the volume stored in the EPR, Eq. 1 was used.

$$V_m = (V_{m-1} + EN_m) - (A_m + E_m) \tag{3}$$

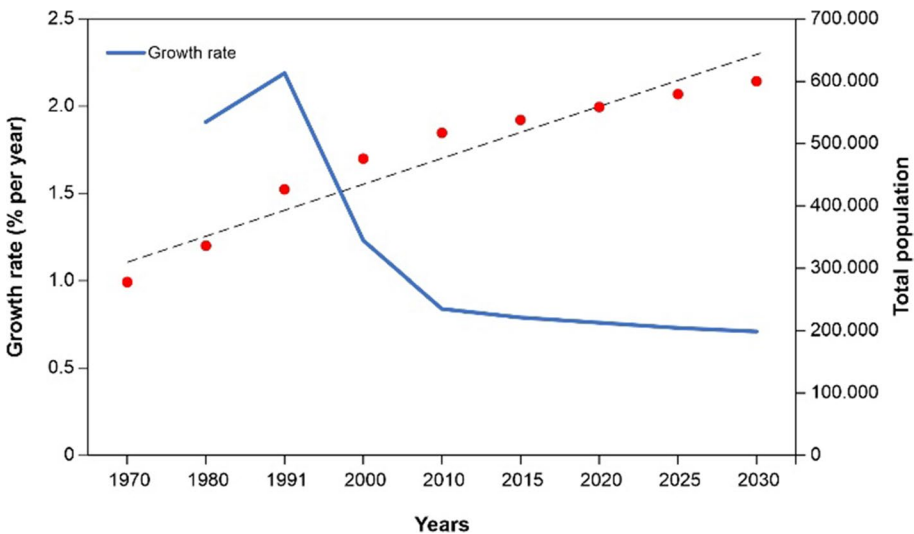


Fig. 6 Urban population between 1970 and 2010, estimated urban population between 2011 and 2030 and growth rate from 1980 to 2030 in the EPR basin

Table 3 Area of types of LULC and variation in the basin and results of the comparison between the estimated LULC and that observed for 2015

LULC	2000	2010	2015	Variation 2000–2015	Prediction 2015	Prediction 2030	Prediction error 2015/2015
	(km ²)			(%)	(km ²)		(%)
Caatinga vegetation	5861.43	6607.16	5795.31	− 1.1	5299.50	5300.72	− 8.56
Agriculture/pasture	7083.07	6231.20	7085.42	0.03	7576.89	7413.2	6.94
Built-up area	323.9	349.31	406.3	25.4	412.00	452.8	1.40
Barren soil	258.07	258.25	258.46	0.6	275.00	278.90	6.40
Water bodies	301.14	382.08	282.9	− 6.1	265.00	382.8	− 6.33

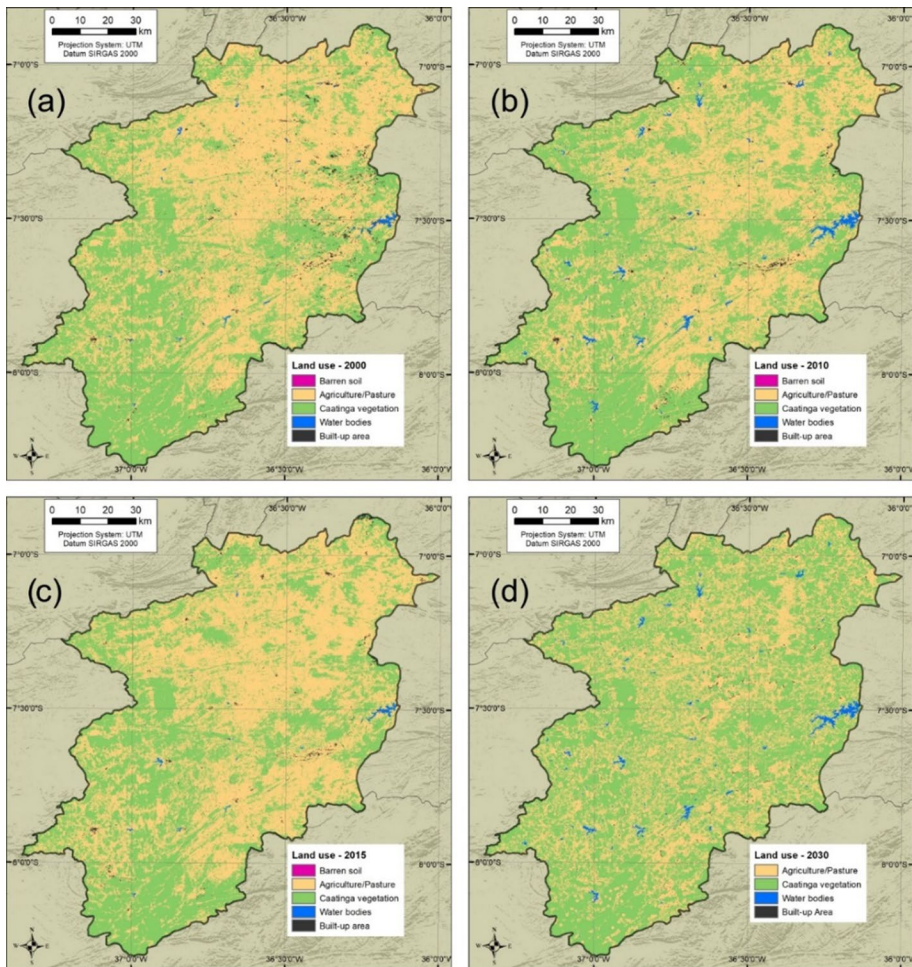


Fig. 7 LULC maps of the EPR basin for **a** 2000, **b** 2010, **c** 2015 and **d** 2030

where V_m is the estimated water volume, V_{m-1} is the water volume stored in the previous month, EN_m is the tributary streamflow in the reservoir in the current month, A_m is the volume of water withdrawn for the public supply in the current month, and E_m is the monthly water loss through evaporation.

3 Results and discussion

3.1 Population projections for the period from 2020 to 2030

Figure 6 shows the adjusted model for the estimated urban population between 1970 and 2030 for the municipalities supplied by the EPR. This figure also shows the population growth rate over time in the EPR basin. The results showed that the model was well adjusted ($R^2=0.92$) and that the data showed a deceleration in the population growth rate in the region after 2010; however, the results show that the population should double between 1970 and 2030. The results showed that the variation in population growth increased 2% from 1970 to 1980, 2.4% from 1980 to 1991, 1.1% from 1991 to 2000, and 0.8% from 2000 to 2010, while the estimated values for the period from 2015 to 2030 varied between 0.9% and 0.8%, which confirmed the growth of the population, although in a less marked way than occurred in the 1980s and 1990s. This behavior follows a trend in Brazil because, even with large population indices, the Brazilian population has shown a decrease in its birth rates and greater longevity of the population (de Espindola et al. 2017).

3.2 Evolution and prediction of LULC

The relative areas of each LULC class for 2000, 2010 and 2015 are shown in Table 3. The LULC maps of these years were analyzed to explore the LULC changes and the associated

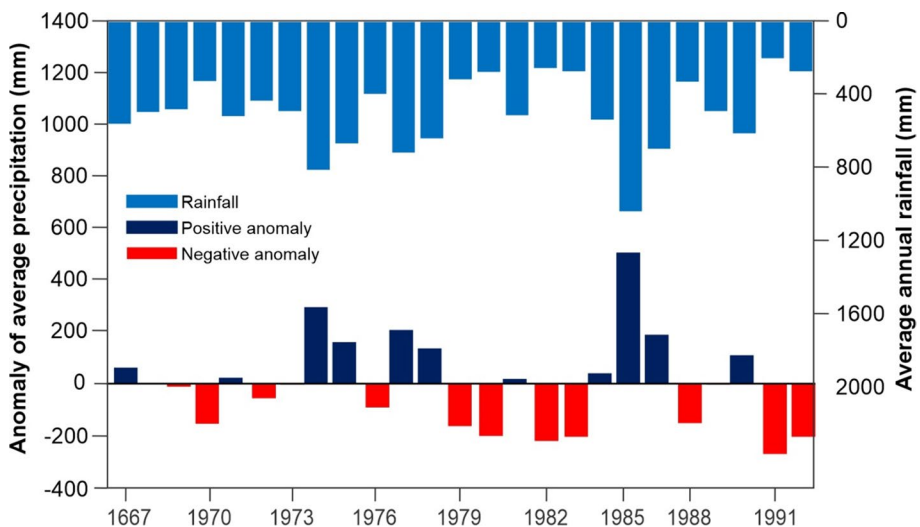


Fig. 8 Anomaly of average precipitation in the EPR basin

impacts on the water resources. Figures 7a, c show the LULC maps for the EPR basin from 2000, 2010 and 2015. In general, it was found that there was an increasing human influence in the EPR basin from the growth of urban areas and a decrease in the Caatinga vegetation areas. The results showed that in the 2000–2015 period, the Caatinga vegetation class was transformed into settlements in the downstream areas. At the same time, the built-up area showed a considerable increase (25.4% between 2000 and 2015), whereas agriculture/pasture area slightly increased. Similar trends continued in the following years with barren soil and water classes, where the development of these classes expanded little in the basin. In total, during the 2000–2015 period, the increase in deforestation augmented by reducing Caatinga vegetation area was approximately 1.1% due to climate variability (Santos et al. 2019b). However, it is worth highlighting that this region is very dynamic because the vegetation depends on climatic conditions and suffers a lot from anthropic influence in the region, which depends on mineral resources and plant extraction (Ferreira da Silva et al. 2020).

Figure 7d shows the spatial distribution of the LULC prediction for 2030. Then, a comparison was made between the LULC map provided by the LCM and the MapBiomass use map for 2015 (Table 3). The results show that the values obtained can be considered satisfactory, with the largest errors ranging from 31% to –19%. The 2030 prediction results pointed to an increase in the Caatinga vegetation area and a decrease in the agriculture/pasture area. There were also increases in the classes of built-up area and water bodies. The increase in built-up area corroborated the results of the population projections, which pointed to an increase in the number of inhabitants. With regard to the water bodies, the results followed what was shown on the map for 2010, which was a rainy year.

3.3 Future rainfall projections for the period from 2020 to 2030

Figure 8 shows the anomaly in the average monthly rainfall in the EPR basin. These results showed that this region suffers from alternating very dry years and rainy years, as noted by Dantas et al. (2020). This high climatic variability in the region combines with factors such as geology and soil types to favor water scarcity and affect the behavior of reservoir volumes (Silva et al. 2020b). According to Dantas et al. (2020), water availability in northeastern Brazil is highly dependent on rain. In the case of EPR, the water security that the reservoir provides can supply the dependent population for approximately four years with below average rainfall, as occurred between 2012 and 2017, when the volume of water stored in the reservoir reached the lowest recorded level, leading to a collapse in the water supply of the region.

This period of scarcity brought a serious water crisis in the region, mainly in the municipality of Campina Grande, and caused multiple socioeconomic problems (Lucena 2018);

Table 4 Statistical analysis of observed (1978–1991) and projected rainfall

Precipitation scenarios	Annual average rainfall (mm)	Mean deviation of rainfall (mm)	Standard deviation of rainfall (mm)
Average observed rainfall	556.36	139.98	186.33
Scenario 1	282.33	113.22	148.75
Scenario 2	258.80	103.79	136.36
Scenario 3	235.27	94.35	123.96

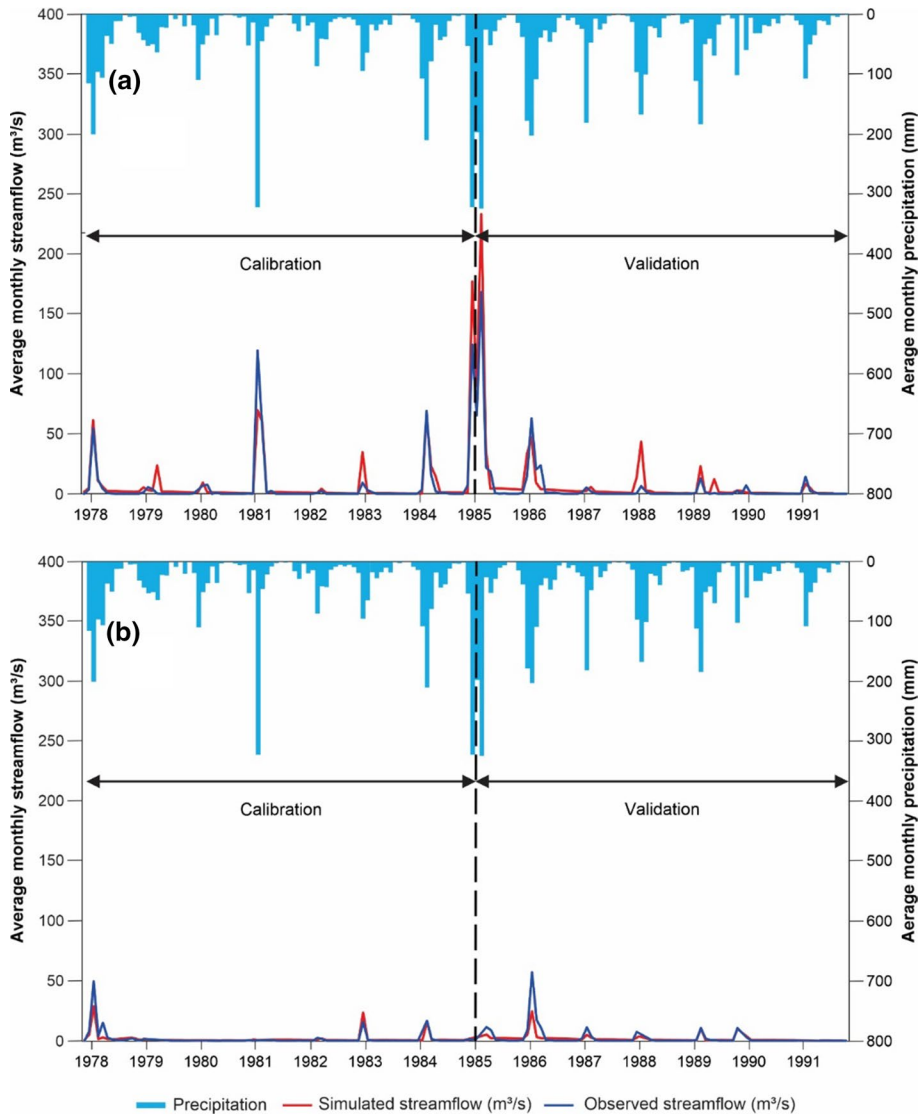


Fig. 9 Results of the streamflow calibration and validation for the stations **a** Caraúbas and **b** Poço de Pedras

it is considered one of the longest drought periods recorded in the history of the region (Cunha et al. 2018). The proposed scenarios represented the recurrence of consecutive dry years in the basin and the impacts that these scenarios could have on the water supply for the region's population. Thus, in terms of severity and subsequent impacts, the drought from 2012 to 2017 can be considered one of the most severe in the history of the region (Marengo et al. 2018), which has provoked new discussions on public policies for managing droughts at the federal and state levels (Dantas et al. 2020).

Table 4 presents the values of the average, average deviation, and standard deviation of the annual rainfall observed in the period between 1981 and 1991 and the projected

Table 5 Statistical analysis of the SWAT calibration and validation

Statistics	Caraúbas		Poço de Pedras	
	Calibration	Validation	Calibration	Validation
	1978–1988	1989–1991	1978– 988	1989–1991
R^2	0.88	0.53	0.79	0.97
Nash	0.8	0.13	0.67	0.95
PBIAS	- 32.04	- 64.5	21.27	- 23.71
Simulated average streamflow (m ³ /s)	9.47	2.03	1.92	1.12
Observed average streamflow (m ³ /s)	7.17	1.23	2.44	0.91

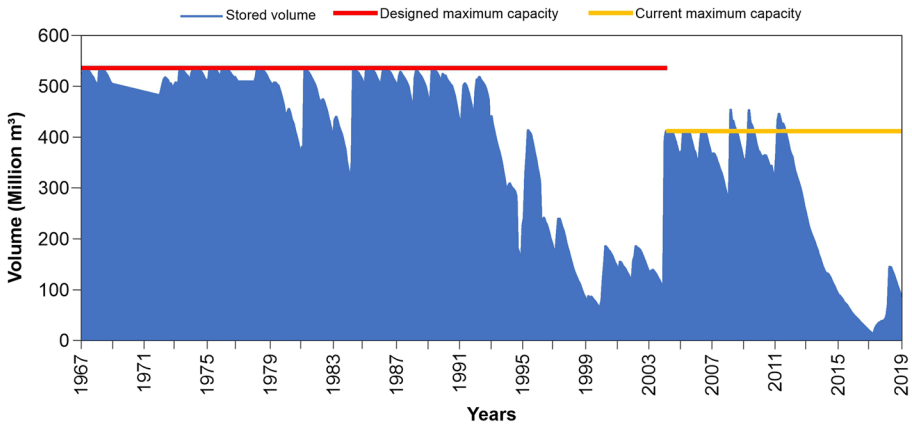


Fig. 10 Observed monthly volumes in the EPR

scenarios for the period from 2020 to 2030. It can be seen in Table 4 that, as in the observed precipitation in the period between 1981 and 1991, the projected precipitation also presented low values and that even with a reduction in the utilized volume, the extreme event existed in all projections.

3.4 Hydrological modeling: calibration, validation and statistical analysis of the performance

The results of the SWAT-CUP automatic calibration can be seen in Figs. 9a, b, which show the observed and calculated streamflow curves for the periods of calibration and validation of the Caraúbas and Poço de Pedras stations, respectively. Figure 9a shows that the model was able to perform a satisfactory streamflow simulation in relation to the streamflow observed during the calibration period. Table 5 shows the results of the statistical analyses of the calibration and validation of the two stations. The modeling results show R^2

and Nash values that are considered good, despite presenting an underestimation, as seen in the PBIAS assessment. In the validation period, however, the results were not as good, although the average observed and simulated values were similar.

The good simulation results were repeated when the results for the Poço de Pedras station (Fig. 9b and Table 5) were analyzed, including the underestimation of the streamflow. However, in this case, the results of the validation period were better than those in the calibration period. This result can be explained by the absence of observed data to make a better comparison between the observed and simulated values.

3.5 Analysis of the volume observed in the Epitácio Pessoa reservoir

Figure 10 shows the monthly behavior of the accumulated volume of the EPR for the period from 1967 to 2019 (AESA 2019). It was observed that the reservoir had a high variability in the stored volume; in some years, it reached maximum capacity (2004, 2006, 2008, 2009 and 2010), while in others, it had low volume (1999, 2003, 2011, 2012, 2013, 2014, 2015, 2016 and 2017). As it is located in a region with a hot and dry climate and the lowest total rainfall in the country, the reservoir is quite vulnerable to climatic variability and anthropic impacts, such as the construction of dams along the main course, which cause the reservoir to go through constant periods of imminent collapse, either in terms of the amount of water available or the quality of water in the region's supply system.

It was noted that starting in 2011, there was a continuous reduction in the stored volume until February 2017, when it reached the lowest level since the construction of the reservoir. Starting in March 2017, the arrival of the water transfer from the São Francisco River began with the PISF. However, even with the PISF water transfer, other problems have been impairing its functionality, making it necessary to interrupt the flow, such as the high evaporation in the region, which reaches approximately 2000 mm/year (De Medeiros et al. 2019), unauthorized withdrawal of water along the canal and on the reservoir margins by numerous agricultural properties (Brito 2013), and problems in the construction of the structure of the PISF canal (Segundo Neto and Vianna 2016).

The reservoir has a storage capacity to withstand stressful situations, which are recurrent. For example, at the end of 2016 and begin of 2017, the EPR reached a stored volume of around 5% of its storage capacity. This fact caused severe social and economic losses to hundreds of thousands of people and several industries that depend on this water. During 2012–2017 period, all the reservoirs within the region dried up, causing serious impacts on the BSAR economy, as highlighted in Alvalá et al. (2019). According to Dantas et al. (2020), the federal government acted to alleviate this crisis by making available public resources for social assistance programs, such as special credit lines and water distribution

Table 6 Observed average (1978–1991) and projected monthly streamflow in the EPR

Rainfall scenarios	Average streamflow	Average streamflow deviation (m^3/s)	Streamflow standard deviation
Observed average	4.14	6.58	16.31
Scenario 1	3.07	2.32	3.23
Scenario 2	2.81	2.21	2.94
Scenario 3	2.57	2.11	2.67

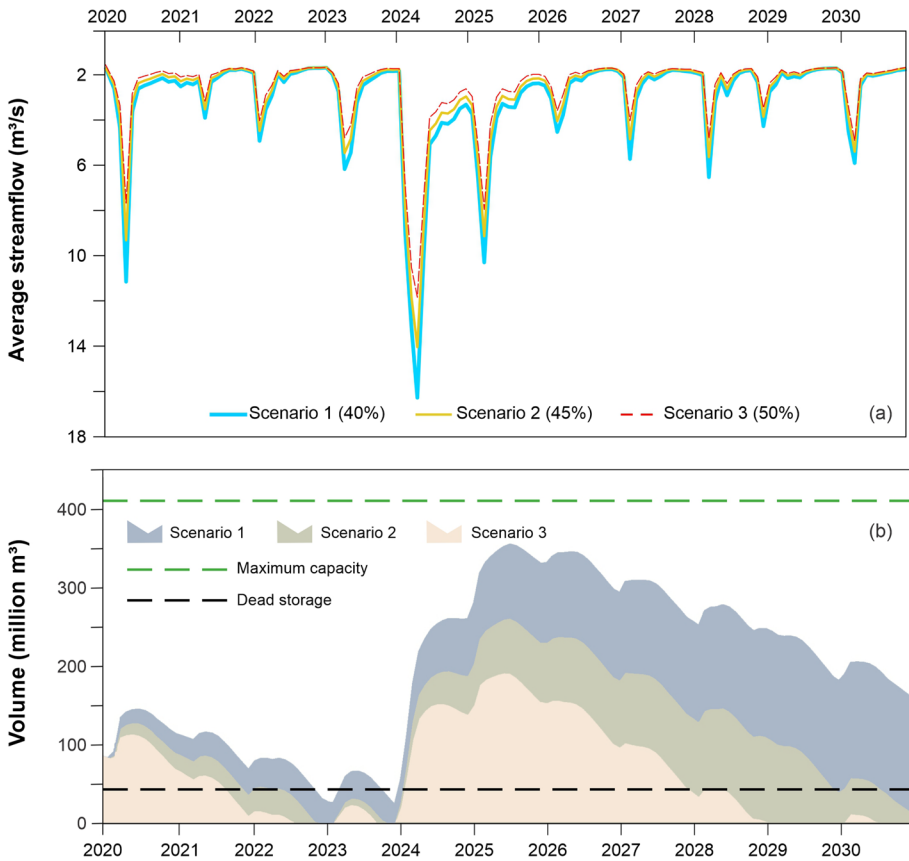


Fig. 11 **a** Temporal distribution of affluent streamflow in the EPR that were projected with the three scenarios, and **b** forecasting scenarios for the volume stored in the EPR in the period between 2020 and 2030

using water tank trucks. These actions did not solve the problem, but only alleviated the critical situation of water supply in the region, which started to carry out extensive water rationing, mainly in Campina Grande city.

3.6 Modeling the projected streamflow and future simulation of the volume stored in the EPR

After calibrating and validating the model, simulations were performed on the SWAT for each future precipitation scenario, thus generating the simulated monthly streamflow between 2020 and 2030. The average estimated values can be seen in Table 6. Figure 11a shows the temporal distribution of the projected affluent flows of the EPR with reductions of 40, 45 and 50% in rainfall that were generated with the SWAT model. It can be seen in this figure that the streamflow peaked in February 2024, which reflected the occurrence of an extreme event.

The results show the values that will be needed to supply the municipalities served by the reservoir. These values represent the monthly consumption that should be captured by

CAGEPA, and it considers the number of inhabitants and a percentage of losses due to system failures. It should be noted that this estimate does not differentiate the use of water, only the collection by the company responsible for supply. The values refer to the volume that should be collected monthly in each year of the projection and are expressed in cubic meters. Subsequently, the results of the population projections were analyzed, generating the projection of demand for human supply, taking into account the values of consumption per capita adopted by CAGEPA, which were indicated in the State Water Resources Plan of the Paraíba State (AESÁ 2018). This study adopted a consumption of 250 L per inhabitant per day and considered that the projections established for the study indicated that the basin should supply a population of more than 600,000 inhabitants.

After adding all the necessary factors, a graph was created with the future volumes that the reservoir will be able to store (Fig. 11b) according to the procedures adopted in this research. In Fig. 11b, the maximum storage capacity of the reservoir was plotted, as was the critical volume, also called dead volume, at which the water quality is compromised by the concentration of salts. The results plotted in this figure demonstrate that starting in 2020, the reservoir will be able to increase its stored volume. However, as soon the process of emptying begins, the reservoir will reach the dead volume between 2021 and 2022 in the most pessimistic scenarios, in which the rainfall was reduced by 45% and 50%, and could even dry out. In the less pessimistic scenario (40% reduction in rainfall), the reservoir would reach the dead volume in two time periods: in 2022 and at the end of 2023.

In 2024, an extreme rainfall event was projected to occur, causing a considerable increase in the volume of the reservoir, reaching a value of 350 million cubic meters in 2025, when it would return to emptying continuously due to the decrease in rainfall. It can be seen when analyzing the graph that the reservoir reached almost its maximum capacity with the continuous streamflow of the PISF. However, this demonstrates that the municipalities supplied by the reservoir cannot be considered safe with respect to water availability, as promised by the project. In addition, the volume of the EPR depends on above-average rainfalls to ensure water supply from above the dead volume. This fact demonstrates the need for a better resource management process with more effective control of water withdrawals, reduction in waste and cultural change in the population to avoid future problems.

As suggestion, further studies could include longer time series of rainfall, streamflow and meteorological, as well as LULC images with higher precision and accuracy to better identify the LULC classes within the BSAR. This information can improve even more the accuracy of the estimates. In addition, integration between SWAT model and remotely sensing data could be considered as well.

4 Conclusions

This research was able to evaluate how and how much the climatic variability, population increase and alterations in the LULC affect the water availability of the EPR and attempted to predict how long the reservoir will be able to meet the population's demand. The hydrological modeling performed for the basin obtained results considered satisfactory during the calibration period, as indicated in the literature. Regarding the generated rainfall scenarios, it can be concluded that the percentages of decrease used in the generation of future flows added to the average flows of the water transfer from São Francisco effectively

represented the temporal variability obtained in the historical series, which reflected periods of increase in the volume. However, rainfall also showed a constant decrease, leading to a decrease in the volume and, consequently, the availability of water in the reservoir.

It can be concluded that the population growth forecast for the period from 2020 to 2030 resulted in a significant increase in the number of inhabitants, which could lead to a collapse in the availability of water in the reservoir in various scenarios of reduced rainfall; population growth will increase the demand for water, even with the water transfer from São Francisco River. The results of this research indicate the hypothesis that even with water transfer, the reservoir will once again enter a critical state, i.e., reach the dead volume, as soon as 2022. The reservoir could reach the dead volume again, and even dry out completely, under the 45% or 50% rainfall reduction scenarios. In this sense, it should be noted here that this is not an accurate forecast, but it aims to alert decision makers about the estimated volume behavior under different climatic and LULC scenarios in the hydrographic basin of the EPR.

This finding raises the need for better management of the reservoir's water resources to avoid a collapse in the water supply system, which would directly affect the populations of the municipality of Campina Grande and all others supplied by the EPR. In addition, it is concluded that PISF is responsible for water supplies in the region, and that the completion of this project and its maintenance are vital to guarantee the availability of water to the population of Campina Grande.

Authors' contributions JFCBCS and RMS designed the research; JFCBCS, RMS and CAGS wrote the original draft; AMS, PCGV, RMS and CAGS performed the manuscript review and editing; CAGS and RMS provided funding acquisition, project administration and resources; and RMS, CAGS, JFCBCS, AMS and PCGV wrote the final paper.

Funding This study was financed in part by the Brazilian Federal Agency for the Support and Evaluation of Graduate Education (Coordenação de Aperfeiçoamento de Pessoal de Nível Superior—CAPES)—Fund Code 001, the National Council for Scientific and Technological Development, Brazil—CNPq (Grant Nos. 304213/2017-9 and 304540/2017-0) and the Federal University of Paraíba.

Availability of data and material The data that support the findings of this study are available from the corresponding author upon reasonable request.

Declarations

Conflict of interest The authors declare that they have no competing interests.

References

- Abbaspour KC, Yang J, Maximov I, Siber R, Bogner K, Mieleitner J, Zobrist J, Srinivasan R (2007) Modelling hydrology and water quality in the pre-alpine/alpine Thur watershed using SWAT. *J Hydrol* 333(2–4):413–430. <https://doi.org/10.1016/j.jhydrol.2006.09.014>
- Abbaspour KC, Rouholahnejad E, Vaghefi S, Srinivasan R, Yang H, Kløve B (2015) A continental-scale hydrology and water quality model for Europe: calibration and uncertainty of a high-resolution large-scale SWAT model. *J Hydrol* 524:733–752. <https://doi.org/10.1016/j.jhydrol.2015.03.027>
- AESA—Agência Executiva de Gestão de Águas do Estado da Paraíba (2018). Relatório final consolidado do PERH-PB. <http://www.paraiba.pb.gov.br/aesa>. Accessed in: 3 December 2018
- AESA—Agência Executiva de Gestão de Águas do Estado da Paraíba (2019). Volume diário dos principais reservatórios. Available at: <http://www.aesa.pb.gov.br>. Accessed: 5 May 2019

- Alvalá RCS, Cunha APMA, Brito SSB, Seluchi ME, Marengo JA, Moraes OLL, Carvalho MA (2019) Drought monitoring in the Brazilian semiarid region. *An Acad Bras Ciênc* 91(Suppl. 1):e20170209. <https://doi.org/10.1590/0001-3765201720170209>
- Alvares CA, Stape JL, Sentelhas PC, de Moraes Gonçalves JL, Sparovek G (2013) Köppen's climate classification map for Brazil. *Meteorol Z* 22(6):711–728. <https://doi.org/10.1127/0941-2948/2013/0507>
- ANA—Agência Nacional de Águas (2018). Rede Hidrometeorológica Nacional. Available at: <https://www.snirh.gov.br/hidroweb>. Accessed in: 5 November 2018
- Anand J, Gosain AK, Khosa R (2018) Prediction of land use changes based on Land Change Modeler and attribution of changes in the water balance of Ganga basin to land use change using the SWAT model. *Sci Total Environ* 644:503–519. <https://doi.org/10.1016/j.scitotenv.2018.07.017>
- Andrade CWL, Montenegro SMGL, Montenegro AAA, Lima JRS, Srinivasan R, Jones CA (2018) Soil moisture and discharge modeling in a representative watershed in northeastern Brazil using SWAT. *Ecohydrol Hydrobiol* 19:238–251. <https://doi.org/10.1016/j.ecohyd.2018.09.002>
- Arnold JG, Srinivasan R, Mutiah RS, Williams JR (1998) Large area hydrologic modeling and assessment part I: model development. *J Am Water Resour As* 34:73–89
- Bacalhau J, Ribeiro Neto A, Montenegro SMGL (2016) Water supply reservoir operation in relation to climate variability: Pirapama River basin (Pernambuco-Brazil). *J Urb Environ Eng* 10(2):279–287. <https://doi.org/10.4090/juee.2016.v10n2.279287>
- Bendini HN, Fonseca LMG, Schwieder M, Körting TS, Rufin P, Sanches IDA, Leitão PJ, Hostert P (2019) Detailed agricultural land classification in the Brazilian cerrado based on phenological information from dense satellite image time series. *Int J Appl Earth Obs Geoinf* 82:101872. <https://doi.org/10.1016/j.jag.2019.05.005>
- Beuchle R, Grecchi RC, Shimabukuro YE, Seliger R, Eva HD, Sano E, Achard F (2015) Land cover changes in the Brazilian Cerrado and Caatinga biomes from 1990 to 2010 based on a systematic remote sensing sampling approach. *Appl Geogr* 58:116–127. <https://doi.org/10.1016/j.apgeog.2015.01.017>
- Braga ACFM, Silva RM, Santos CAG, Galvão CO, Nobre P (2015) Downscaling of a global climate model for estimation of runoff, sediment yield and dam storage: a case study of Pirapama basin, Brazil. *J Hydrol* 498:46–58. <https://doi.org/10.1016/j.jhydrol.2013.06.007>
- Brasil (2004) Projeto de Integração do Rio São Francisco com bacias hidrográficas do nordeste setentrional: relatório de impacto ambiental—RIMA. Ministério da Integração Nacional, Brasília, p 2004
- Brasil Neto RM, Santos CAG, Silva JFCBC, Silva RM, Santos CAC, Mishra M (2021) Evaluation of the TRMM product for monitoring drought over Paraíba State, northeastern Brazil: a trend analysis. *Sci Rep* 11:286–296. <https://doi.org/10.1038/s41598-020-80026-5>
- Brasil (2021) Projeto Rio São Francisco—O andamento das obras. <https://www.gov.br/pt-br/noticias/transito-e-transportes/2020/08/integracao-do-sao-francisco-chegara-ao-cinturao-das-aguas-do-ceara>. Accessed 17 Mar 2021
- Brito FB (2013) Conflitos pelo acesso e uso da água: integração do Rio São Francisco com a Paraíba (Eixo Leste). Programa de Pós-Graduação em Geografia, Tese de Doutorado, UFRGS, Porto Alegre, Brasil, p 371
- Brito CS, Silva RM, Santos CAG, Brasil Neto RM, Coelho VHR (2021) Monitoring meteorological drought in a semiarid region using two long-term satellite-estimated rainfall datasets: a case study of the Piranhas River basin, northeastern Brazil. *Atmos Res* 250:105380. <https://doi.org/10.1016/j.atmosres.2020.105380>
- Calijuri ML, de Castro JS, Costa LS et al (2015) Impact of land use/land cover changes on water quality and hydrological behavior of an agricultural subwatershed. *Environ Earth Sci* 74:5373–5382. <https://doi.org/10.1007/s12665-015-4550-0>
- Celeste AB, Billib M (2009) Evaluation of stochastic reservoir operation optimization models. *Adv Water Resour* 32(9):1429–1443. <https://doi.org/10.1016/j.advwatres.2009.06.008>
- Coelho VHR, Bertrand GF, Montenegro SMGL, Paiva ALR, Almeida CN, Galvão CO, Barbosa LR, Batista LFDR, Ferreira ELGA (2018) Piezometric level and electrical conductivity spatiotemporal monitoring as an instrument to design further managed aquifer recharge strategies in a complex estuarine system under anthropogenic pressure. *J Environ Manag* 209:426–439. <https://doi.org/10.1016/j.jenvman.2017.12.078>
- Cunha APMA, Tomasella J, Ribeiro-Neto GG, Brown M, Garcia SR, Brito SB, Carvalho MA (2018) Changes in the spatial-temporal patterns of droughts in the Brazilian Northeast. *Atmos Sci Lett* 19:e855. <https://doi.org/10.1002/asl.855>
- Dantas JC, Silva RM, Santos CAG (2020) Drought impacts, social organization and public policies in northeastern Brazil: a case study of the Upper Paraíba River basin. *Environ Monit Assess* 192:317. <https://doi.org/10.1007/s10661-020-8219-0>

- de Espindola GM, Carneiro ELNC, Façanha AC (2017) Four decades of urban sprawl and population growth in Teresina. *Braz Appl Geogr* 79(1):73–83. <https://doi.org/10.1016/j.apgeog.2016.12.018>
- de Medeiros IC, da Costa SJFCB, Silva RM, Santos CAG (2019) Run-off-erosion modelling and water balance in the Epitácio Pessoa Dam river basin, Paraíba State in Brazil. *Int J Environ Sci Technol* 33:545–562. <https://doi.org/10.1007/s13762-018-1940-3>
- Dos Santos CAC, Mariano DA, Nascimento FCA, Dantas FRC, Oliveira G, Silva MT, da Silva LL, da Silva BB, Bezerra BG, Safa B, Medeiros SS, Neale CMU (2020) Spatio-temporal patterns of energy exchange and evapotranspiration during an intense drought for drylands in Brazil. *Int J Appl Earth Obs Geoinf* 85:101982. <https://doi.org/10.1016/j.jag.2019.101982>
- Eastman JR (2016) Manual IDRISI TerrSet: geospatial monitoring and modeling system. Clark Labs, Worcester, p 393
- EMBRAPA (2018) – Empresa Brasileira de Pesquisa Agropecuária. Sistema de Informação de Solos Brasileiros
- Ferreira da Silva GJ, De Oliveira NM, Santos CAG, da Silva RM (2020) Spatiotemporal variability of vegetation due to drought dynamics (2012–2017): a case study of the Upper Paraíba River basin, Brazil. *Nat Hazards* 102:939–964. <https://doi.org/10.1007/s11069-020-03940-x>
- Golmohammadi G, Rudra R, Dickinson T, Goel P, Veliz M (2017) Predicting the temporal variation of streamflow contributing areas using SWAT. *J Hydrol* 547:375–386. <https://doi.org/10.1016/j.jhydrol.2017.02.008>
- IBGE—Instituto Brasileiro de Geografia e Estatística (2021). Cidades@ <https://www.ibge.gov.br/cidades-e-estados/pb/campina-grande.html>. Accessed 28 Mar 2021
- INMET—Instituto Nacional de Meteorologia (2018) Banco de Dados Meteorológicos para Ensino e Pesquisa. Available at: <http://www.inmet.gov.br/porta/index.php?r=bdmep/bdmep>. Accessed in: 15 December 2018
- Islam K, Rahman MF, Jashimuddin M (2018) Modeling land use change using cellular automata and artificial neural network: the case of Chunati Wildlife Sanctuary, Bangladesh. *Ecol Indic* 88:439–453. <https://doi.org/10.1016/j.ecolind.2018.01.047>
- Khawaldah HA (2016) A prediction of future land use/land cover in Amman area using GIS based Markov model and remote sensing. *J Geogr Inf Syst* 8(3):412–427. <https://doi.org/10.4236/jgis.2016.83035>
- Liebertrau AM (1983) Measures of association. Sage Publications, Newbury Park (**Quantitative**)
- Lucena DPMM (2018) simulações da implantação de ações de gestão no açude Epitácio Pessoa e seus impactos na crise hídrica em Campina Grande-PB e região. Programa de Pós-Graduação em Engenharia Civil e Ambiental, Dissertação de Mestrado, UFCG, Campina Grande, Brasil, p 94
- MapBiomass (2019a) Collection 4.0 of Brazilian land cover and use map series. <http://mapbiomas.org/en>
- MapBiomass (2019b) Collection 4.0 of Brazilian land cover and use map series: accuracy analysis. <https://mapbiomas.org/en/accuracy-analysis>
- Marçal NA, da Silva RM, Santos CAG, dos Santos JS (2019) Analysis of the environmental thermal comfort conditions in public squares in the semiarid region of northeastern Brazil. *Build Environ* 152:145–159. <https://doi.org/10.1016/j.buildenv.2019.02.016>
- Marengo JA, Alves LM, Alvalá RCS, Cunha AP, Brito S, Moraes OLL (2018) Climatic characteristics of the 2010–2016 drought in the semiarid northeast Brazil region. *An Acad Bras Ciênc*. <https://doi.org/10.1590/0001-3765201720170206>
- Martins VS, Kaleita A, Barbosa CCF, Fassoni-Andrade AC, Lobo FL, Novo EMLM (2019) Remote sensing of large reservoir in the drought years: implications on surface water change and turbidity variability of Sobradinho reservoir (Northeast Brazil). *Remote Sens Appl Soc Environ* 13:275–288. <https://doi.org/10.1016/j.rsase.2018.11.006>
- Mas J-F, Kolb M, Paegelow M, Olmedo MTC, Houet T (2014) Inductive pattern-based land use/cover change models: a comparison of four software packages. *Environ Model Softw* 51(1):94–111. <https://doi.org/10.1016/j.envsoft.2013.09.010>
- Millington JDA, Katerinchuk V, da Silva RFB, Victoria DC, Batistella M (2021) Modelling drivers of Brazilian agricultural change in a telecoupled world. *Environ Model Softw* 139:105024. <https://doi.org/10.1016/j.envsoft.2021.105024>
- Moriasi DN, Arnold JG, Van Liew MW, Bingner RL, Harmel RD, Veith TL (2007) Model evaluation guidelines for systematic quantification of accuracy in watershed simulations. *Trans ASABE* 50(3):885–900. <https://doi.org/10.13031/2013.23153>
- Nash JE, Sutcliffe JV (1970) River streamflow forecasting through conceptual models part I-A discussion of principles. *J Hydrol* 10(3):282–290. [https://doi.org/10.1016/0022-1694\(70\)90255-6](https://doi.org/10.1016/0022-1694(70)90255-6)
- Neto FVAS, Vianna PCG (2016) Análise espacial das obras do projeto de integração do rio São Francisco-PISF (Eixo Leste) no estado da Paraíba. *Geo UERJ* 28:219–241. <https://doi.org/10.12957/geouerj.2016.14536>

- Oliveira GM, Leitão MMVBR, Galvão CO, Leitão TJV (2005) Estimativa da evaporação e análise do uso do coeficiente (Kp) do tanque “Classe A” nas regiões do Cariri e Sertão da Paraíba. *Rev Bras Recur Hídric* 10(4):73–83
- Olmedo MTC, Pontius Junior RG, Paegelow M, Mas J-F (2015) Comparison of simulation models in terms of quantity and allocation of land change. *Environ Model Softw* 69:214–221. <https://doi.org/10.1016/j.envsoft.2015.03.003>
- Parente L, Ferreira L, Faria A, Nogueira S, Araújo F, Teixeira L, Hagen S (2017) Monitoring the Brazilian pasturelands: a new mapping approach based on the Landsat 8 spectral and temporal domains. *Int J Appl Earth Obs Geoinf* 62:135–143. <https://doi.org/10.1016/j.jag.2017.06.003>
- Pereira DR, Martínez MA, Silva DD (2016) Hydrological simulation in a basin of typical tropical climate and soil using the SWAT Model Part II: simulation of hydrological variables and soil use scenarios. *J Hydrol Reg Stud* 5:149–163. <https://doi.org/10.1016/j.ejrh.2016.05.0020>
- Pereira TS, Costa DD, Fragoso Junior C, Montenegro SMGL, Bertacchi Uvo C (2018) Key climate oscillation factors controlling precipitation variability during the dry season in eastern Northeast Brazil: study case of Mundaú and Paraíba do Meio river basins. *Water* 10:1617. <https://doi.org/10.3390/w10111617>
- Pes MP, Pereira EB, Marengo JA, Martins FR, Heinemann D, Schmidt M (2017) Climate trends on the extreme winds in Brazil. *Renew Energy* 109:110–120. <https://doi.org/10.1016/j.renene.2016.12.101>
- Santos CAG, Brasil Neto RM, da Silva RM, Costa S (2019a) Cluster analysis applied to spatiotemporal variability of monthly precipitation over Paraíba state using tropical rainfall measuring mission (TRMM) data. *Remote Sens* 11(6):637–655. <https://doi.org/10.3390/rs11060637>
- Santos CAG, Brasil Neto RM, Silva RM, dos Santos D (2019b) Innovative approach for geospatial drought severity classification: a case study of Paraíba state, Brazil. *Stoch Env Res Risk Assess* 33(2):545–562. <https://doi.org/10.1007/s00477-018-1619-9>
- Santos JYG, Montenegro SMGL, Silva RM, Santos CAG, Quinn NW, Dantas APX, Ribeiro Neto A (2021) Modeling the impacts of future LULC and climate change on runoff and sediment yield in a strategic basin in the Caatinga/Atlantic forest ecotone of Brazil. *CATENA*. <https://doi.org/10.1016/j.catena.2021.105308>
- SEMARH—Secretaria Extraordinária do Meio Ambiente, dos Recursos Hídricos e Minerais do Estado da Paraíba (2004) Resultados do levantamento batimétrico do reservatório Epitácio Pessoa, Boqueirão/PB. SEMARH/LMRS, Campina Grande, p 2004
- Silva JFCBC (2019) Crise hídrica no abastecimento de água em Campina Grande: análise de cenários futuros no volume de água do reservatório Epitácio Pessoa entre 2020 e 2030. Ph.D. Thesis in Geography, Federal University of Paraíba, p 122
- Silva RM, Santos CAG, Maranhão KUA, Silva AM, Lima VRP (2018a) Geospatial assessment of eco-environmental changes in desertification area of the Brazilian semi-arid region. *Earth Sci Res J* 22:175–186. <https://doi.org/10.15446/esrj.v22n3.69904>
- Silva RM, Dantas JC, Beltrão JA, Santos CAG (2018b) Hydrological simulation in a tropical humid basin in the Cerrado biome using the SWAT model. *Hydrol Res* 49(3):908–923. <https://doi.org/10.2166/nh.2018.222>
- Silva LP, Dantas APX, Silva RM, Santos CAG (2020a) Modeling land cover change based on an artificial neural network for a semiarid river basin in northeastern Brazil. *Global Ecol Conserv* 21:503–519. <https://doi.org/10.1016/j.scitotenv.2018.07.017>
- Silva RM, Silva JFCBC, Santos CAG, Silva AM, Brasil Neto RM (2020b) Spatial distribution and estimation of rainfall trends and erosivity in the Epitácio Pessoa reservoir catchment, Paraíba, Brazil. *Nat Hazards* 101:765–785. <https://doi.org/10.1007/s11069-020-03926-9>
- Souza BI, Suertegaray DMA, Lima ERV (2009) Desertificação e seus efeitos na vegetação e solos do Cariri Paraibano. *Mercator* 8(16):217–232. <https://doi.org/10.4215/RM2009.0816.0017>
- Tian W, Liu X, Wang K, Bai P, Liu C (2021) Estimation of reservoir evaporation losses for China. *J Hydrol* 596:26142. <https://doi.org/10.1016/j.jhydrol.2021.126142>
- Tomasella J, Vieira RMSP, Barbosa AA, Rodríguez DA, de Oliveira Santana M, Sestini MF (2018) Desertification trends in the Northeast of Brazil over the period 2000–2016. *Int J Appl Earth Obs Geoinf* 73:197–206. <https://doi.org/10.1016/j.jag.2018.06.012>
- Umar IA, Negash BM, Quainoo AK, Ayoub MA (2021) An outlook into recent advances on estimation of effective stimulated reservoir volume. *J Nat Gas Sci Eng* 88:103822. <https://doi.org/10.1016/j.jngse.2021.103822>
- Wang Y, Ziv G, Adami M, Mitchard E, Batterman SA, Buerman W, Marimon BS, Marimon Junior BH, Reis SM, Rodrigues D, Galbraith D (2019) Mapping tropical disturbed forests using multi-decadal 30 m optical satellite imagery. *Remote Sens Environ* 221:474–488. <https://doi.org/10.1016/j.rse.2018.11.028>

- Wu S-J, Kuo C-Y, Yeh K-C, Wang C-D, Wang W-J (2021) Reliability analysis for reservoir water supply due to uncertainties in hydrological factors, rainfall-runoff routing and operating rule curves. *J Hydro-environment Res* 34:24–45. <https://doi.org/10.1016/j.jher.2021.01.002>
- Xie W, Huang Q, He C, Zhao X (2018) Projecting the impacts of urban expansion on simultaneous losses of ecosystem services: a case study in Beijing, China. *Ecol Ind* 84:183–193. <https://doi.org/10.1016/j.ecolind.2017.08.055>
- Yao H, Georgakakos A (2001) Assessment of Folsom Lake response to historical and potential future climate scenarios: 2. Reservoir management. *J Hydrol* 249(1–4):176–196. [https://doi.org/10.1016/S0022-1694\(01\)00418-8](https://doi.org/10.1016/S0022-1694(01)00418-8)

Publisher's Note Springer Nature remains neutral with regard to jurisdictional claims in published maps and institutional affiliations.